

Stacking Faults and Their Effect on Magnetocrystalline Anisotropy in Co and Co-Alloy Thin Films

Bo Bian, Wei Yang, David E. Laughlin, and David N. Lambeth

Abstract—Stacking faults in $(10\bar{1}0)$ uniaxial Co and Co-alloy thin films have been analyzed by the electron diffraction technique. As predicted no diffraction contrast of stacking faults could be observed when the beam is parallel to the $[10\bar{1}0]$ direction. However, both by plan-view TEM observation and electron diffraction along the $[11\bar{2}0]$ direction reveal that the stacking fault density in biased pure Co $(10\bar{1}0)$ thin films is much lower than that in unbiased ones. The addition of Cr in Co films significantly reduces stacking fault density whereas the addition of 8at% Pt leads to a considerable increase in stacking fault density. Our results show that stacking faults in Co thin films significantly, and negatively, affect the anisotropy energy density and its temperature dependence.

Index Terms—Anisotropy, Co-alloy thin films, electron diffraction, magnetic recording, stacking faults, TEM.

I. INTRODUCTION

THE RECENT increase in areal density of magnetic recording is placing very stringent requirements in magnetocrystalline anisotropy energy of Co-alloys. It is directly related to the maximum achievable coercivity and thermal stability of recorded data. The hcp structure of Co has an ABAB atomic arrangement along the $\langle 0001 \rangle$ direction, which can be easily changed to ABCABC stacking during the deposition process due to the small energy difference between these two stacking arrangements [1]. When the ABC stacking occurs in the hcp structure it is called a stacking fault. Stacking faults in Co-alloy magnetic media have been investigated by diffraction contrast imaging [2], high-resolution transmission electron microscopy [3]–[5] and grazing incidence x-ray scattering using synchrotron radiation [6]. Although intensive research efforts have been undertaken with the purpose of improving the recording properties, the effects of stacking faults on the magnetic properties such as coercivity are still controversial due to the difficulty in quantitatively characterizing stacking fault density and separating the effects of stacking faults from other influences such as grain size, composition and orientation [4], [7]–[9]. Hence, knowledge of the effects of stacking faults

on anisotropy constants is essential for the development of high density Co-alloy media. It is advantageous to have a thin film system in which both the stacking faults and anisotropy constants can be directly characterized.

We previously found that $(10\bar{1}0)$ Co uniaxial (the c -axes of the Co crystals are aligned at one direction) films could be epitaxially grown on sputter deposited Cr templates epitaxially grown as Cr(112)/Ag(110) on hydrofluoric acid etched Si (110) substrates [10]. The single, in-plane easy axis orientation of these Co grains allows the direct determination of the anisotropy constants by torque or hard axis hysteresis measurements. In this work, we observed and characterized stacking faults in uniaxial $(10\bar{1}0)$ pure Co films sputtered with and without substrate biasing, and we correlate the stacking fault density with the magnetocrystalline anisotropy constant and the anisotropy constant temperature dependence. We also investigate the change of stacking fault density with Cr and Pt additions in Co alloys.

II. EXPERIMENTAL

Ag, Cr and Co or Co-alloy thin films were sequentially deposited onto HF-etched Si (110) substrates by rf diode sputtering in a Leybold–Heraeus Z-400 system. The etched Si wafers were heated to about 300 °C under vacuum prior to film deposition. The thicknesses of the Ag, Cr and Co or Co-alloy thin films were 75, 50 and 50 nm, respectively. Pure Co films were deposited with and without -300 V substrate bias. $\text{Co}_{80}\text{Cr}_{20}$ and $\text{Co}_{92}\text{Pt}_8$ targets were used to deposit Co-alloy thin films without substrate biasing in order to maintain composition. TEM samples were prepared by mechanical polishing and dimpling followed by ion milling from the Si substrate side. Microstructural analyzes were performed using a Philips EM-420 electron microscope operating at 120 kV. Magnetocrystalline anisotropy constants were determined by measuring both hard axis hysteresis loops and torque curves.

III. RESULTS AND DISCUSSION

The $(10\bar{1}0)$ zone axis TEM image and corresponding ED pattern of a pure Co uniaxial film grown on Cr/Ag/HF-Si (110) is shown in Fig. 1. The uniaxial nature of the $(10\bar{1}0)$ Co film can be seen from the ED pattern. As can be predicted no fringes from stacking faults are visible in the image and none of the reflections in the ED pattern show streaks. To explain the diffraction mechanism, calculation of the structure factors of a perfect hcp structure with only AB sequence and an hcp structure

Manuscript received October 13, 2000.

This work was supported by IBM and the Data Storage Systems Center at Carnegie Mellon University under Grant ECD-89-07068 from the National Science Foundation.

B. Bian, W. Yang, and D. N. Lambeth are with the Electrical and Computer Engineering Department, Carnegie Mellon University, Pittsburgh, PA 15213 USA (e-mail: {bbian; lambeth}@ece.cmu.edu; wy28@stanford.edu).

D. E. Laughlin is with the Materials Science and Engineering Department, Carnegie Mellon University, Pittsburgh, PA 15213 USA (e-mail: dl0p+@andrew.cmu.edu).

Publisher Item Identifier S 0018-9464(01)07320-4.

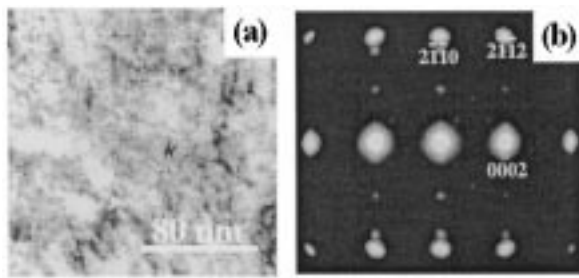


Fig. 1. $[10\bar{1}0]$ zone axis TEM image and corresponding ED pattern of a $(10\bar{1}0)$ uniaxial Co film. No fringes and streaks are visible.

containing local ABC stacking must be understood. The difference in diffraction intensities of a perfect hcp crystal and a faulted hcp crystal depends on the indices of the diffraction planes [11]. When $h - k = 3n$, where n is an integer, the diffraction intensity of a faulted region is the same as that of a perfect one since both regions have the same structure factor. When $h - k = 3n \pm 1$, however, the presence of stacking faults results in a modified diffraction intensity distribution along the direction of the (0002) reflection due to the difference in the structure factors of both regions. The intensity distribution results in streaks in the electron diffraction pattern. As all the reflections of Co in the $[10\bar{1}0]$ zone axis ED pattern have the indices satisfying $h - k = 3n$, no streaks exist in the ED patterns regardless of the existence of stacking faults.

As the $[11\bar{2}0]$ zone axis electron diffraction of a hcp structure contains reflections satisfying $h - k = 3n \pm 1$, and since this zone axis is only 30 degrees away from the $[10\bar{1}0]$ zone axis, we can tilt TEM samples of $(10\bar{1}0)$ Co uniaxial films 30 degrees around the c axes and observe the samples along their $[11\bar{2}0]$ zone axes. Fig. 2 shows the TEM images and corresponding ED patterns of pure Co uniaxial films deposited without bias, (a), and with -300 V substrate bias, (b). Dense parallel fringes perpendicular to the $[0001]$ direction are observed in both TEM images. Long and bright streaks as marked by arrows are clearly visible in the ED patterns. These streaks form almost continuous and parallel straight lines extending along the direction of the (0001) reflections. Kinematically forbidden reflections such as (0001) , (0003) , etc., appear in the ED patterns due to double diffraction. The TEM image and ED pattern in Fig. 2(a) were taken from the same region as shown in Fig. 1(a). The only difference is the choice of zone axis for observation. This result shows that high-density stacking faults may exist in $(10\bar{1}0)$ textured Co films but can only be observed by diffraction contrast imaging and electron diffraction along selected special zone axes. From the TEM images in Fig. 2, it is seen that the stacking fault density value for the Co film prepared without bias is much greater than that of the Co sample prepared with -300 V bias. Also, streaks in the ED patterns in Fig. 2(a) appear to be more obvious as compared with that in Fig. 2(b).

The introduction of Pt and/or Cr into Co not only results in a different chemical composition; these added atoms may also alter the film microstructure. Fig. 3 shows the $[11\bar{2}0]$ zone axes TEM images and ED patterns of $\text{Co}_{80}\text{Cr}_{20}$ (a) and $\text{Co}_{92}\text{Pt}_8$ (b) uniaxial films. Similar to those of the pure Co films, streaks are observed in the ED patterns and fringes are visible in the images. As compared with pure Co film deposited without substrate

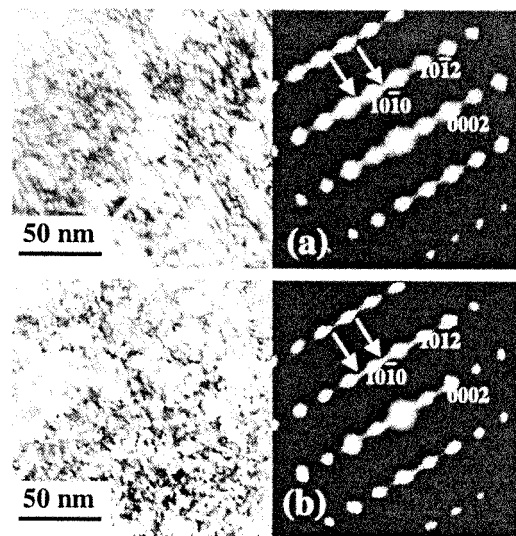


Fig. 2. $[11\bar{2}0]$ zone axis TEM images and corresponding ED patterns of the uniaxial pure Co films deposited without bias (a) and with -300 V bias (b). Fringes and streaks are visible. The difference in stacking fault densities with the use of bias is obvious.

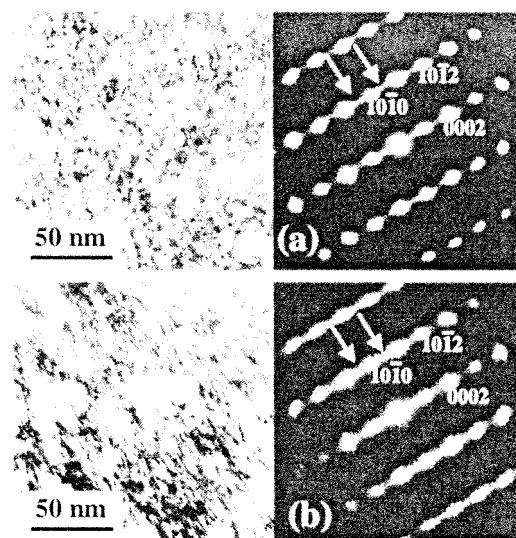


Fig. 3. $[11\bar{2}0]$ zone axis TEM images and corresponding ED patterns of $(10\bar{1}0)$ $\text{Co}_{80}\text{Cr}_{20}$ (a) and $\text{Co}_{92}\text{Pt}_8$ (b) uniaxial films.

bias, the $\text{Co}_{80}\text{Cr}_{20}$ film shows a smaller stacking fault density. Since the misfit at the interfaces of $\text{Cr}\backslash\text{Co}$ and $\text{Cr}\backslash\text{CoCr}$ are almost the same and Cr is a bcc material, the difference may result from chemical effect of Cr.

In order to quantitatively compare the stacking fault densities of different samples, it is necessary to characterize the diffraction intensity distribution. For this purpose diffraction patterns obtained from $2 \mu\text{m}$ diameter large regions in the TEM samples were recorded with a Gatan CCD camera with a constant gain reference. The exposure time was chosen so as not to cause over exposure at the peaks of intensities of interest. Generally the stacking faults in polycrystalline hcp materials cause peak broadening in the x-ray diffraction. The broader the peak, the higher the stacking fault density. A similar effect happens in electron diffraction. When there is a larger peak broadening, the intensity is distributed across a wider range, and hence the intensity in the midpoint between two electron diffraction spots

TABLE I
COMPARISON OF STACKING FAULT GENERATED NORMALIZED INTENSITY OF STREAKS I_{streaks} AND ANGULAR PEAK WIDTH δ

Materials	Co	Co (-300 V)	Co ₉₂ Pt ₈	Co ₈₀ Cr ₂₀
I_{streaks}	0.17	0.09	0.24	0.05
δ (rad)	0.13	0.09	0.18	0.07
α (rad)	0.15	0.11	0.20	0.09
β (rad)	0.07	0.06	0.09	0.06

is higher. We measured the diffraction intensities at $(10\bar{1}1/2)$ and $(10\bar{1}-1/2)$ reflections as shown by arrows and normalized their average intensity by the intensity of the $(10\bar{1}0)$ reflection. The normalized intensity of streaks, I_{streak} , is used to compare stacking fault density in our samples. Similar to the method used in the x-ray diffraction, we also used peak broadening along the (0001) direction of the electron diffraction spots to characterize the stacking fault density. However, the peak broadening due to the angular dispersion of the in-plane lattice axis alignment and the instrumental broadening should also be considered. The peak width of the $(10\bar{1}0)$ reflection, for example, contains contributions from the stacking faults in addition to the dispersion and instrumental broadening, while for the (0004) reflection, the peak broadening perpendicular to (0001) direction contains no contribution from the streaks. Hence, the combined dispersion and instrumental broadening can be estimated by measuring the width of the (0004) peak along the axis perpendicular to the streaking direction. More specifically, the angular peak width of the (0004) spot, β , is defined as the measured width/reciprocal vector length of (0004) . Similarly, the angular peak width of the $(10\bar{1}0)$ spot, α , is equal to the measured width/reciprocal vector length of the $(10\bar{1}0)$ spot. Assuming the intensity distributions due to these broadening mechanisms are Gaussian functions, the intensity profile of the spot reflections will be a convolution of the individual broadened distributions. Consequently, the stacking fault resulted broadening is $\delta = (\alpha^2 - \beta^2)^{1/2}$. Table I shows the relative intensity of the streaks and the peak broadening among uniaxial films of Co and Co-alloys. From the table, it can be seen that these materials can be arranged in the following order according to decreasing stacking fault density of the corresponding uniaxial films:

$$\text{Co}_{92}\text{Pt}_8 > \text{Co} > -300 \text{ V biased Co} > \text{Co}_{80}\text{Cr}_{20}.$$

Our electron diffraction analysis demonstrates that substrate biasing is an effective way to reduce the stacking fault density in Co films. Also, alloy composition can significantly influence the stacking fault density. The addition of Cr significantly reduces stacking fault density in Co-alloy thin films. The decrease of stacking fault density with Cr addition is not surprising as Cr generally destabilize the fcc structure in Co alloys. The increase of stacking fault density with Pt addition may be due to the fcc tendency of Pt and larger misfit at the Cr/CoPt interface.

The temperature dependences of anisotropy constants K_1 of $(10\bar{1}0)$ uniaxial pure Co films without bias and with -300 V substrate bias are shown in Fig. 4. The K_1 values of the Co films were determined by fitting the measured hard axis magnetic hysteresis loops [12]. The K_1 of the Co films deposited at -300 V bias is larger than those of the unbiased Co films. The K_1 of the biased Co films becomes zero at approximately 240°C whereas

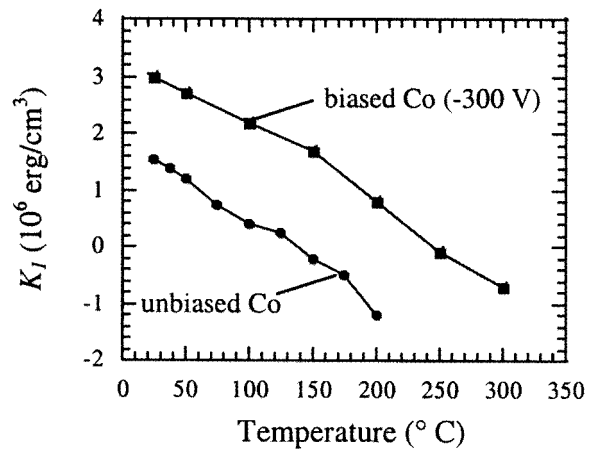


Fig. 4. Temperature dependences anisotropy constants K_1 of $(10\bar{1}0)$ uniaxial pure Co films without bias and with -300 V substrate bias.

the K_1 of the unbiased Co films reaches zero around 140°C . Since our x-ray diffraction did not show significant difference in lattice constants in the two films ($<0.4\%$ in a ; $<0.2\%$ in c), the higher stacking fault density is most probably the cause for the lower anisotropy.

IV. CONCLUSION

Both TEM observation and electron diffraction revealed that the stacking fault density in biased pure Co $(10\bar{1}0)$ thin films is lower than that in unbiased ones. The addition of Cr in Co films can significantly reduce stacking fault density whereas the addition of 8 at% Pt leads to a considerable increase in stacking fault density. Our results show that stacking faults in Co and Co alloy thin films significantly, and negatively, affect the anisotropy.

REFERENCES

- [1] B. E. Warren, *X-ray Diffraction*. New York: Dover, 1990.
- [2] K. Hono, B. G. Demczyk, and D. E. Laughlin, "Electron microdiffraction of faulted regions in Co-Cr and Co-Ni-Cr thin films," *Appl. Phys. Lett.*, vol. 55, pp. 229-231, 1989.
- [3] T. P. Nolan, R. Sinclair, R. Ranjan, and T. Yamashita, "Effect of microstructural features on media noise in longitudinal recording media," *IEEE Trans. Magn.*, vol. 28, pp. 3258-3260, 1992.
- [4] B. Y. Wong, Y. Shen, and D. E. Laughlin, "An investigation on the fine defect structure of CoCrTa/Cr magnetic thin films," *J. Appl. Phys.*, vol. 73, pp. 418-421, 1993.
- [5] A. Ishikawa and R. Sinclair, "Analysis of stacking fault density in Co-alloy thin films by high-resolution electron microscopy," *IEEE Trans. Magn.*, vol. 32, pp. 3605-3607, 1996.
- [6] P. Dova, H. Laidler, K. O'Grady, M. F. Toney, and M. F. Doerner, "Effects of stacking faults on magnetic viscosity in thin film magnetic recording media," *J. Appl. Phys.*, vol. 85, pp. 2775-2777, 1999.
- [7] S. Duan, M. R. Khan, J. E. Haeefe, L. Tang, and G. Thomas, "Magnetic property and microstructure dependence of CoCrTa/Cr media on substrate temperature and bias," *IEEE Trans. Magn.*, vol. 28, pp. 3258-3260, 1992.
- [8] P. Glijer, J. M. Sivertsen, and J. H. Judy, "Effects of platinum content and substrate bias on the structure and magnetic properties of CoCrPt/Cr thin films," *J. Appl. Phys.*, vol. 73, pp. 5563-5565, 1993.
- [9] S. E. Mckinlay, N. Fussing, R. Sinclair, and M. Doerner, "Microstructure/magnetic property relationships in CoCrPt magnetic thin films," *IEEE Trans. Magn.*, vol. 32, pp. 3605-3607, 1996.
- [10] W. Yang, D. N. Lambeth, and D. E. Laughlin, "Uniaxial Co-alloy media on Si (110) ," *J. Appl. Phys.*, vol. 85, pp. 4723-4725, 1999.
- [11] H. Blank, P. Delavingnette, R. Gevers, and S. Amelinckx, "Fault structures in wurtzite," *Phys. Stat. Sol.*, vol. 7, pp. 747-764, 1964.
- [12] B. D. Cullity, *Introduction to Magnetic Materials*. Reading, MA: Addison-Wesley, 1972.